

PACS numbers: 87.50.W–; 87.57.C–; 87.63.lt
DOI: 10.1070/QE2014v044n08ABEH015543

Laser speckle contrast imaging of skin blood perfusion responses induced by laser coagulation

M. Ogami, R. Kulkarni, H. Wang, R. Reif, R.K. Wang

Abstract. **We report application of laser speckle contrast imaging (LSCI), i.e., a fast imaging technique utilising backscattered light to distinguish such moving objects as red blood cells from such stationary objects as surrounding tissue, to localise skin injury. This imaging technique provides detailed information about the acute perfusion response after a blood vessel is occluded. In this study, a mouse ear model is used and pulsed laser coagulation serves as the method of occlusion. We have found that the downstream blood vessels lacked blood flow due to occlusion at the target site immediately after injury. Relative flow changes in nearby collaterals and anastomotic vessels have been approximated based on differences in intensity in the nearby collaterals and anastomoses. We have also estimated the density of the affected downstream vessels. Laser speckle contrast imaging is shown to be used for high-resolution and fast-speed imaging for the skin microvasculature. It also allows direct visualisation of the blood perfusion response to injury, which may provide novel insights to the field of cutaneous wound healing.**

Keywords: *laser speckle contrast imaging, laser coagulation, blood perfusion, skin.*

1. Introduction

Blood vessels play an important and complex role in wound healing. For instance, blood vessels function to re-establish haemostasis and mediate cell migration during inflammation stage [1]. Moreover, sufficient oxygen supply in the form of haemoglobin in the blood supply is necessary for rapid closure of the wound [2]. While the broad mechanism behind the wound healing process has been defined, little is understood about the changes in the microvasculature of the skin near the injury site [3]. Even less is known about how perfusion changes within the seconds after injury occurs. Moreover, limited knowledge of blood perfusion in the skin has led to only partial understanding of why skin diseases such as psoriasis and the cutaneous effects of diabetes occur and how they may be more permanently remedied, resulting in only temporary alleviation in the form of topical creams or medication [4]. Additionally, an understanding of rapid perfusion responses to injury may aid studies in enhancing the wound healing process. To better study the microvascular responses to injury, a fast-response imaging system with good image resolution is needed. Current imaging systems have insufficient resolution to capture small microvasculature, require the injection of a contrast agent, and/or take minutes to collect data [5–7].

Recently, attention has been placed on a promising imaging technique known as laser speckle contrast imaging (LSCI), which uses the random interference pattern produced by coherent interference between photons backscattered from different tissue constituents to track moving objects, such as the red blood cells within the vessels. The image resolution can be high enough to image arterioles and some capillaries, which makes it superior to ultrasound imaging [8]. Moreover, the LSCI system is fast, simple, affordable and noninvasive, making it ideal for repeated *in vivo* studies [9]. LSCI has been used to study burn scar perfusion, monitor cerebral blood flow and image retinal blood flow [7, 10, 11]. It has also been employed to image blood coagulation in paper [12], where use was made of mechanical occlusion and laser injury to study clot development. Kalchenko et al. [12] also observed that long-exposure LSCI is capable of imaging lymph and blood vessels [13]. Multimodal imaging combining fluorescence microscopy with LSCI has also been used to visualise lymph and blood vessels, which was then applied by Kuznetsov et al. [14] to study the permeability of blood vessels. More recently, Tripathi et al. [15] have utilised LSCI to measure coagulation metrics through alterations in the rate of speckle intensity fluctuations caused by a clot. In order to find how the microvasculature responds to local injury, an injury model which can accurately target on a selected artery without changing the local environment should be established. Attempts to study the change in the vasculature due to injury have been made using various techniques such as manually pressing the vessel [11]. However, excess pressure may cause the vessel to rupture. Moreover, it may cause unnecessary occlusion of other vessels which can give inaccurate results. Another option to induce injury would be using a biopsy punch, which has been done by Jung et al. [16]. They explored long-term healing on the scale of days using optical microangiography [17–20], but this method results in a permanent tissue damage and fails to target only one selected vessel. Laser coagulation is a technique where coagulation is achieved by exposing tissue to multiple high-energy light pulses with a repetition rate determined by a Q-switch in a nanosecond laser system. Multiple pulses allow for cooling to occur in between pulses, resulting in a high light dosage to the vessel while reducing the amount of damage to surrounding tissue structures [21]. Laser coagulation has been previously used with ultrasound techniques for tracking the changes in placental perfusion while studying the effects of maternal haemodynamics having the twin-to-twin transfusion

M. Ogami, R. Kulkarni, H. Wang, R. Reif, R.K. Wang Department of Bioengineering, University of Washington, 3720 15th Avenue NE, Seattle, Washington 98195, USA; e-mail: wangrk@uw.edu

Received 1 April 2014; revision received 15 June 2014
Kvantovaya Elektronika **44** (8) 746–750 (2014)
Submitted in English

syndrome [22]. However, the image resolution of ultrasound systems is insufficient to accurately visualise acute changes after a laser coagulation procedure. Laser coagulation has also been utilised together with an optical coherence gated imaging system to observe changes associated in an *in vitro* porcine cornea [23]. However, there was no information about how microvasculature responds to laser coagulation. Therefore, with the fast response and relatively high image resolution, the laser coagulation procedure in combination with laser speckle contrast imaging may provide novel insights to fast microvasculature responses to local injury.

An important component of LSCI is the processing of the data. Traditional laser speckle calculates speckle contrast using the formula [24]:

$$K_t(x,y) = \frac{\sigma_t(x,y)}{\langle I(x,y)\rangle}. \quad (1)$$

Here, K_t is the temporal contrast at a given pixel, σ_t is the standard deviation of the pixel intensity over time and $\langle I(x,y)\rangle$ is the mean light intensity. Liu et al. [23] proposed a new method of contrast calculation that enhances motion contrast. In this method, the ratio in pixel intensity between consecutive frames is taken and the standard deviation is calculated from those ratios, enhancing the contrast between moving speckles and the background.

Using this processing method in conjunction with a compact LSCI system and a laser coagulation module will allow the instant perfusion response after a local injury to be investigated. In this study, the microvasculature flow changes are recorded before, during and after the exposure of the vessel to Nd:YAG laser pulses. Superior image quality is achieved with the processing method. The vessel density and relative flow velocity are calculated to quantify the changes induced by laser coagulation. The results show the capability to track microvascular flow changes in the case of a locally induced injury and may therefore potentially be used to study the cutaneous wound healing process.

2. Materials and methods

2.1. Experimental setup

The scheme of the experimental setup is shown in Fig. 1. The coherent illumination beam from a ~660-nm, 50-mW red diode iFlex-2000 laser (Qioptiq Inc., Rochester, NY, US) was collimated by a lens and passed through a diffuser lens to uniformly illuminate the mouse ear examined at an angle of 45° from the tissue normal direction. A neutral-density filter was used to control the light intensity incident on the sample. The resulting light backscattered from the sample was passed through the zoom lens and was then received by the fast metal-oxide semiconductor A504K camera (Basler, Germany). The magnification of the system was adjusted to 1.5× and the field of view (FOV) was set to be 9×5 mm. To obtain optimal laser speckle images, an exposure time of 0.9 ms and a frame rate of 1107.4 frames per second were set for the camera.

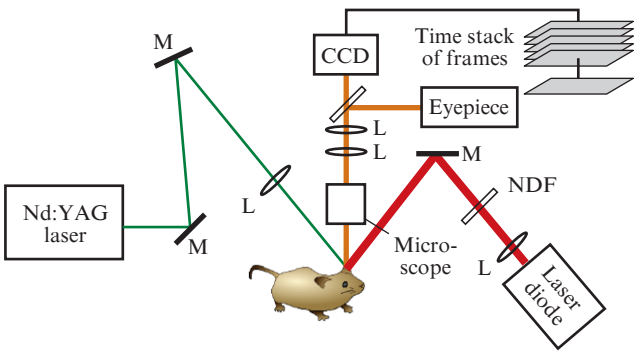

Figure 1. Scheme of the laser coagulation and laser speckle imaging system:
(M) mirror; (L) lens; (CCD) charge-coupled device; (NDF) neutral density filter wheel.

2.2. Animal preparation

To prove the enhanced capability of our method for visualising immediate responses in dynamic blood flow in blood vessels (particularly capillary beds) after injury, we imaged the ear flap on a mouse model. In total, five hairless SKH-1E mice (22 to26 g) (Charles River, Hollister, CA, US) were tested and imaged for this study. For each experiment, the mice were anesthetised with 1.5% isofluorane mixed with 0.2 L min^{-1} oxygen and 0.8 L min^{-1} air by a face mask. The mouse ear was fixed with double-sided tape with the dorsal side facing upwards onto a stage to minimise motion caused by breathing and heart beats. A thin layer of mineral oil was applied to the ear flap to improve matching of the refractive index of the mouse ear tissue to that of the air. A 532-nm nanosecond pulsed Nd:YAG laser (Surelite OPO Plus) was used to perform laser coagulation on the mouse ear. The pulsed laser beam was first targeted at the selected artery using a low energy level (Q-switching, 430 ms). A localised injury in the ear flap was then induced by exposing the pulsed laser light at high energy level (Q-switching, 390 ms) for 30 s to generate a blood clot at the selected artery. The laser speckle images were continuously acquired before, during and after the laser coagulation procedure.

2.3. Image processing

After collecting the camera data, the raw data was processed in MATLAB to create the final picture. First, a time stack of 50 frames was used to determine the intensity ratio between consecutive frames

$$D_i(x,y) = \frac{I_i(x,y)}{I_{i+1}(x,y)},$$

where i is the current frame and $i + 1$ is the next frame. After that, the difference was taken between consecutive division images using the formula [24]:

$$\Delta D_i(x,y) = \frac{D_i(x,y) - D_{i+1}(x,y)}{2}. \quad (2)$$

Speckle contrast was then calculated using the formula:

$$K_t(x,y) = \left(\sum_{i=1}^{N} \frac{\{\Delta D_i(x,y) - \mathrm{mean}[\Delta D(x,y)]\}^2}{N-1}\right)^{1/2}, \quad (3)$$

where N is the total number of frames in one stack. A median filter was then used to reduce some of the background noise.

3. Results

3.1. Tracking blood flow changes

The time frame of this experiment was on the scale of minutes, with data for consecutive frames collected within seconds of each other. For this experiment, time zero corresponds to laser coagulation onset and frames collected before correspond to 'negative time'. The method of image processing used measures discontinuity in motion; therefore, the faster the red blood cells move, the whiter the vessels will appear in the final image. In essence, it focuses on the change in strength of the signal as one blood cell leaves a pixel and is replaced by another. However, when the speed of the red blood cells surpasses the maximum velocity that the LSCI system can track, the signal washes out and the vessel appears black. In this case, the motion discontinuity cannot be tracked because the blood cells move too fast for the signal change to be detected [24]. The baseline image before the laser coagulation procedure is shown in Fig. 2a, where the coagulation target point is labelled as a black dot. Right after exposing to the green Nd:YAG laser pulses (wavelength, 532 nm; peak energy, 65 mJ; and pulse duration, ~3 ns), downstream capillaries (open arrows in Fig. 2b) were much less visible compared to baseline (Fig. 2a). In the meantime, anastomotic vessels (closed arrows in Fig. 2b) appeared much stronger than in the baseline image, indicating a mild occlusion in the targeted artery. With more laser pulses incident on the target area, a more severe occlusion was generated. This can be visualised in Fig. 2c, where the downstream flow (marked as circle) was significantly reduced and became undetectable by the system. Additionally, the flow through the collateral artery below (open arrow in Fig. 2d) increased and anastomotic vessels (closed arrows in Fig. 2d) became apparent in the ischemic region. After stopping the exposure to the pulsed laser energy, higher perfusion was observed in the branch arteries (white arrows in Fig. 2e), which may represent the temporal hyperaemia which is likely to occur right after the recovery of the occlusion. With the temporal blood clot moving away, the affected flow was gradually restored as shown in Fig. 2f.

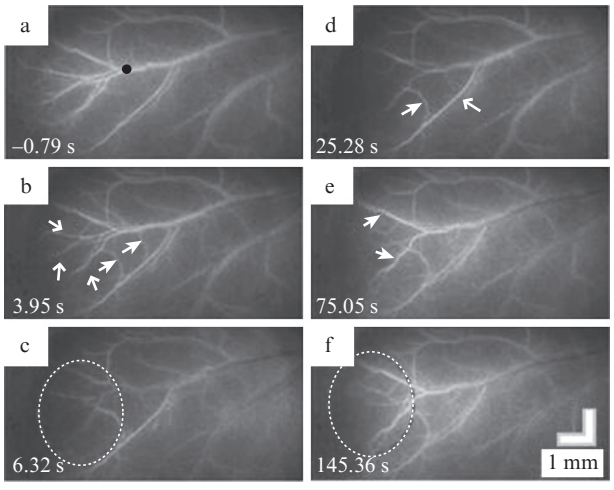

Figure 2. Laser speckle contrast images extracted from a video: (a) image acquired before irradiation by the Nd:YAG laser; (b), (c), (d), (e) and (f) images acquired afterwards at the time points as shown. The Nd:YAG laser light was incident on the mouse ear from 0 to 30 s with a pulse repetition rate of 5 Hz, and the energy at the sample plane was ~1 mJ. The targeted area is labelled with the black dot in Fig. 2a.

3.2. Quantifying relative blood flow velocity changes

Because LSCI does not collect any data pertaining to the velocity distribution, only relative velocities between frames can be calculated, which are difficult to correlate to actual velocities [24]. The change in relative velocity was calculated at five different locations to quantify the changes observed after laser coagulation. The five locations were chosen covering different types of vessels (Fig. 3a). The occluded artery is labelled as a star and marked as A; one branching artery from the occluded artery is labelled as a cross and marked as B; one anastomotic vessel between the occluded artery and its collateral is labelled as a triangle and marked as C; and the two downstream vessels are labelled as a rectangle and a circle and marked as D and E, respectively. Figure 3b shows the changes in the relative blood flow velocity after the laser coagulation procedure. Frames after coagulation refer to the video frames after the green Nd:YAG laser shot its final pulse and the duration of each frame is about 0.79s. There is a sharp peak at roughly 30 s into the experiment in Fig. 3b for all the curves, which was due to the speckle image saturation caused by the strong coagulation laser pulse. At the end of the coagulation procedure, the flow velocity within the occluded artery was decreased (curve A), while the branching arteries above and below the occluded artery showed an increase in velocity (curve B). In the meantime, the supply from the collateral

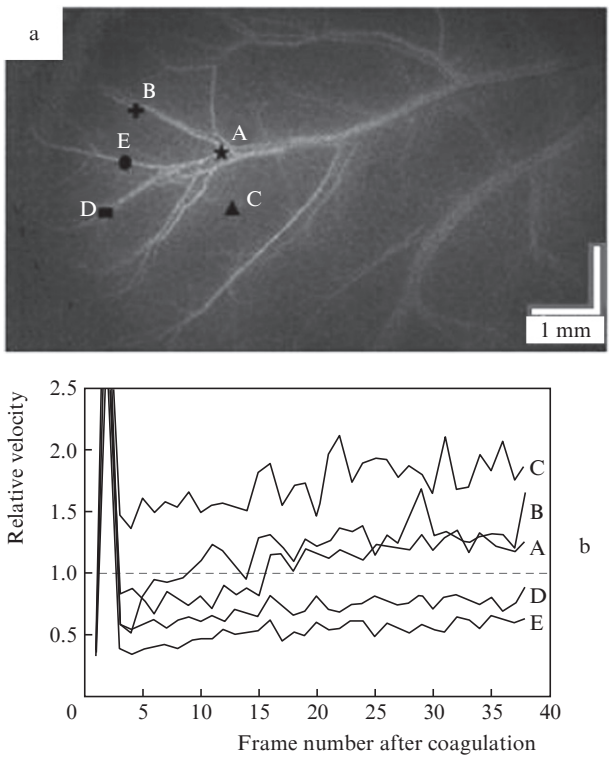

Figure 3. Relative velocity changes over time at different vessels after the laser coagulation procedure: (a) locations at which relative velocities were calculated (C is the point at which the vessel was targeted, B is the occluded vessel, D and E are the downstream vessels and A is the collateral vessel); (b) relative velocity at points A, B, C, D and E after coagulation, respectively.

artery was significantly increased through the anastomotic vessel (triangle in Fig.3a) and the velocity of the anastomotic vessel remained at a ~1.5 times faster velocity compared to the baseline. Blood in the far-end downstream vessels (curves D and E) was flowing slowly at the beginning of the occlusion and did not come back to the velocity before the coagulation.

3.3. Quantifying vessel density changes

To better quantify the microvasculature changes after the laser coagulation procedure, the vessel density has been derived and plotted over time. To calculate the vessel density for each image, a segmentation algorithm is applied. Briefly, images in this method are binarized with an adaptive threshold technique specifically tailored for quantifying small vasculature changes [25], and vessel density is calculated by dividing the number of ones with the total pixel number. Figure 4 shows the changes in vessel density after the laser coagulation procedure. It can be seen that during laser coagulation, the downstream vessel density decreased from about 0.4 to almost 0 after being exposed to the pulsed laser. When the coagulation process was finished, the flow in the occluded artery was restored. An increase in the downstream vessel density of the occlusion site was observed, reaching between 0.2 and 0.15 before the data acquisition ended.

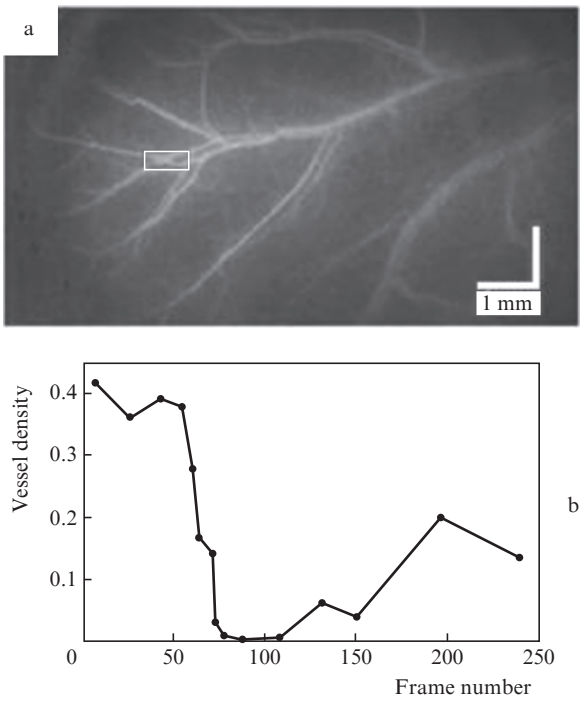

Figure 4. (a) Region of interest (marked with a rectangle) used for vessel density analysis and (b) the vessel density values over the period of data acquisition.

4. Discussion and conclusions

Overall, immediate perfusion changes were detected using the developed LSCI system along with the laser coagulation procedure. Occlusion in the downstream of the targeted artery was instantly observed in the laser speckle images with an increased flow in vessels peripheral to the occluded region. The ability to qualitatively assess changes in the relative velocity and quantitatively plot the vessel density in the region of interest strengthens the potential applications of the developed system. The system setup is compact and low-cost. It can also be easily adapted to other applications, such as laser coagulation induced stroke study on animals. The neutral density filter allows for adjusting the power exposed on the sample, which gives the flexibility to adjust the exposure time to help image vessels with a certain velocity range. Additionally, a longer exposure would allow for better visualisation of the vessels, while a shorter exposure time allows for faster image acquisition and can catch faster blood flow. Changes in microvascular perfusion were well observed through the continuous recording of the occlusion experiment. The main occlusion event seems to occur during laser coagulation exposure. The black appearance in vessels upstream of the clot site seen during photocoagulation indicates that the maximum velocity that the algorithm can handle has been surpassed. The increase in the upstream flow is necessary to compensate for the occluded vessels. In addition, the role of collateral vessels and anastomoses in rescuing the ischemic area has been well recorded in our study. The recovery of the occluded vessels was seen afterward, probably indicating that the clot has been cleared out of the vessel. All these changes were captured by the system just seconds after laser coagulation exposure began.

Figure 3 presents the changes in the relative velocity at the five selected spatial locations A, B, C, D and E. In Fig. 3b, the spike seen initially (between frame 0 and 5) is a result of the oversaturation of green light during laser coagulation. The relative velocity first decreases at A, where the clot is formed. As the artery at C supplies blood to points B, D and E, the relative velocity is seen to decrease at those points too. Due to clot formation (A), the collateral vessel from the nearby artery (C) supplies the vessel while the clot is still at A. This is seen by the increase in relative velocity at A. The random spikes seen at (A) represent random spurts of blood given out as the clot is washed out. These spurts also lead to an increase in blood flow velocity at the artery's lower branches (D and E) and the occluded vessel (B). As the clot gets washed away, the relative velocity at point C decreases as it is no longer required to supply blood to the artery. The relative velocity at all points stabilises after the clot has washed away.

The changes in vessel density confirmed that the flow was diverted to collateral arteries around the clot site, where it was then used to maintain blood flow around the occluded vessels. This diversion of flow can be explained by the increase in pressure caused by blocking the vessel. Because blood volume remains constant, blood that should be travelling through the clot site moves instead to the surrounding vessels that have a lower pressure. The increase in vessel density is observed after photocoagulation has stopped, suggesting that the sudden wash out of the clot released the built up pressure, causing a spurt of blood as flow was restored to the previously occluded downstream vessels.

Our developed LSCI imaging system in combination with the laser coagulation method showed great promise in studying microvascular responses to local injury, which may potentially improve the understanding of wound healing. However, there is still room for improvement, such as increasing the signal-to-noise ratio (SNR), which will eventually help improve the image contrast. One limitation with the current LSCI system is the strong scattering caused by the skin. Various groups have investigated different techniques for reducing scattering caused by biological tissues using topical optical

clearing agents [26–28]. This might be a noteworthy endeavour to improve the overall image quality. Further investigation may be done to define an optimal exposure and sampling rate to produce even better images while still maintaining the ability of visualising fast perfusion changes. It would also be very interesting to study the relationship between the number of pulses incident on the tissue and the coagulation effect. Histological analysis may be needed to analyse whether the surrounding tissue is damaged or not.

References

1. Singer A.J., Clark R.A. *New Engl. J. Med.*, **341**, 738 (1999).
2. Guo S., Dipietro L.A. *J. Dent. Res.*, **89**, 219 (2010).
3. Kirsner R.S., Eaglstein W.H. *Dermatol. Clin.*, **11**, 629 (1993).
4. Raut A.S., Prabhu R.H., Patravale V.B. *Crit. Rev. Ther. Drug Carrier Syst.*, **30**, 183 (2013).
5. Patwari P., Weissman N.J., Boppart S.A., Jesser C., Stamper D., Fujimoto J.G., et al. *Am. J. Cardiol.*, **85**, 641 (2000).
6. Joo C., Kim K.H., de Boer J.F. *Opt. Lett.*, **32**, 623 (2007).
7. Stewart C.J., Frank R., Forrester K.R., Tulip J., Lindsay R., Bray R.C. *Burns.*, **31**, 744 (2005).
8. Boas D.A., Dunn A.K. *J. Biomed. Opt.*, **15**, 011109 (2010).
9. Richards L.M., Kazmi S.M., Davis J.L., Olin K.E., Dunn A.K. *Biomed. Opt. Express*, **4**, 2269 (2013).
10. Dunn A.K., Bolay H., Moskowitz M.A., Boas D.A. *J. Cereb. Blood Flow Metab.*, **21**, 195 (2001).
11. Srienc A.I., Kurth-Nelson Z.L., Newman E.A. *Front Neuroenergetics*, **2**, 128 (2010).
12. Kalchenko V., Brill A., Bayewitch M., Fine I., Zharov V., Galanzha E., et al. *J. Biomed. Opt.*, **12**, 052002 (2007).
13. Kalchenko V., Kuznetsov Y., Meglinski I., Harmelin A. *J. Biomed. Opt.*, **17**, 050502 (2012).
14. Kuznetsov Y.L., Kal'chenko V.V., Meglinski I.V. *Kvantovaya Elektron.*, **41**, 308 (2011) [*Quantum Electron.,* **41**, 308 (2011)].
15. Tripathi M.M., Hajjarian Z., Van Cott E.M., Nadkarni S.K. *Biomed. Opt. Express.*, **5**, 817 (2014).
16. Jung Y., Dziennis S., Zhi Z., Reif R., Zheng Y., Wang R.K. *PLoS One*, **8**, e57976 (2013).
17. Wang R.K., Jacques S.L., Ma Z., Hurst S., Hanson S.R., Gruber A. *Opt. Express*, **15**, 4083 (2007).
18. Wang R.K., Hurst S. *Opt. Express*, **15**, 11402 (2007).
19. Wang R.K., An L., Francis P., Wilson D.J. *Opt. Lett.*, **35**, 1467 (2010).
20. An L., Qin J., Wang R.K. *Opt. Express*, **18**, 8220 (2010).
21. Jia W., Tran N., Sun V., Marincek M., Majaron B., Choi B., et al. *Lasers Surg. Med.*, **44**, 144 (2012).
22. Nizard J., Gussi I., Ville Y. *Ultrasound Obstet. Gynecol.*, **28**, 670 (2006).
23. Liu R., Qin J., Wang R.K. *J. Biomed. Opt.*, **18**, 060508 (2013).
24. Briers D., Duncan D.D., Hirst E., Kirkpatrick S.J., Larsson M., Steenbergen W. et al. *J. Biomed. Opt.*, **18**, 066018 (2013).
25. Reif R., Qin J., An L., Zhi Z., Dziennis S., Wang R. *Int. J. Biomed. Imaging*, **2012**, 509783 (2012).
26. Tuchin V.V., Maksimova I.L., Zimnyakov D.A., Kon I.L., Mavlyutov A.H., Mishin A.A. *J. Biomed. Opt.*, **2**, 401 (1997).
27. Wang R.K., Xu X., Tuchin V.V., Elder J.B. *J. Opt. Soc. Am. B*, **18**, 948 (2001).
28. Jiang J., Boese M., Turner P., Wang R.K. *J. Biomed. Opt.*, **13**, 021105 (2008).